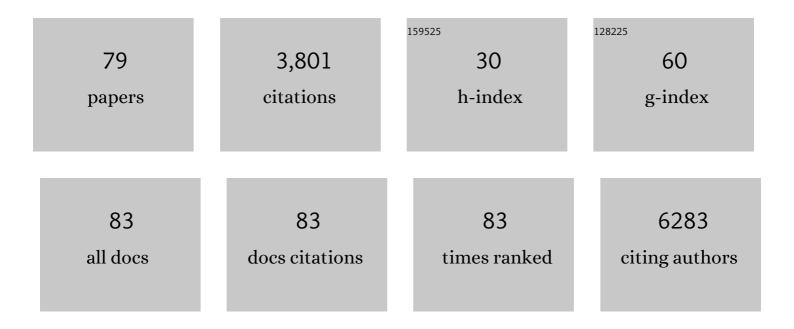
Jiun-Jie Wang

List of Publications by Year in descending order

Source: https://exaly.com/author-pdf/3555630/publications.pdf Version: 2024-02-01



LUIN-LE WANC

#	Article	IF	CITATIONS
1	Diffusion tensor imaging for the differential diagnosis of Parkinsonism by machine learning. Biomedical Journal, 2023, 46, 100541.	1.4	4
2	Deep learning based diagnosis of Parkinson's Disease using diffusion magnetic resonance imaging. Brain Imaging and Behavior, 2022, 16, 1749-1760.	1.1	13
3	Deep Learning–Based Brain Computed Tomography Image Classification with Hyperparameter Optimization through Transfer Learning for Stroke. Diagnostics, 2022, 12, 807.	1.3	15
4	Magnetic Resonance Imaging of Transplanted Porcine Neonatal Pancreatic Cell Clusters Labeled with Exendin-4-Conjugated Manganese Magnetism-Engineered Iron Oxide Nanoparticles. Nanomaterials, 2022, 12, 1222.	1.9	1
5	Noninvasive Tracking of mPEC-poly(Ala) Hydrogel-Embedded MIN6 Cells after Subcutaneous Transplantation in Mice. Polymers, 2021, 13, 885.	2.0	4
6	Fixel-Based Analysis of White Matter Degeneration in Patients With Progressive Supranuclear Palsy or Multiple System Atrophy, as Compared to Parkinson's Disease. Frontiers in Aging Neuroscience, 2021, 13, 625874.	1.7	10
7	Magnetic Resonance Imaging of Transplanted Porcine Neonatal Pancreatic Cell Clusters Labeled with Chitosan-Coated Superparamagnetic Iron Oxide Nanoparticles in Mice. Polymers, 2021, 13, 1238.	2.0	6
8	International Multicenter Analysis of Brain Structure Across Clinical Stages of Parkinson's Disease. Movement Disorders, 2021, 36, 2583-2594.	2.2	54
9	Exendin-4-Conjugated Manganese Magnetism-Engineered Iron Oxide Nanoparticles as a Potential Magnetic Resonance Imaging Contrast Agent for Tracking Transplanted β-Cells. Nanomaterials, 2021, 11, 3145.	1.9	3
10	Functional human brain connectivity during labor and its alteration under epidural analgesia. Brain Imaging and Behavior, 2020, 14, 2647-2658.	1.1	2
11	Prediction of the Clinical Severity of Progressive Supranuclear Palsy by Diffusion Tensor Imaging. Journal of Clinical Medicine, 2020, 9, 40.	1.0	6
12	T1 and T2â^— relaxation time in the parcellated myocardium of healthy Taiwanese participants: AÂsingle center study. Biomedical Journal, 2020, , .	1.4	1
13	Oxygen-sensitive T2* magnetic resonance imaging to correlate heart function and ischemic etiology of post-hospitalized chronic heart failure patients. European Journal of Radiology, 2020, 128, 109036.	1.2	1
14	A Method for the Prediction of Clinical Outcome Using Diffusion Magnetic Resonance Imaging: Application on Parkinson's Disease. Journal of Clinical Medicine, 2020, 9, 647.	1.0	7
15	Left Ventricular Function and Myocardial Triglyceride Content on 3T Cardiac MR Predict Major Cardiovascular Adverse Events and Readmission in Patients Hospitalized with Acute Heart Failure. Journal of Clinical Medicine, 2020, 9, 169.	1.0	9
16	The effect of spatial resolution on the reproducibility of diffusion imaging when controlled signal to noise ratio. Biomedical Journal, 2019, 42, 268-276.	1.4	8
17	Acupuncture Effect and Mechanism for Treating Pain in Patients With Parkinson's Disease. Frontiers in Neurology, 2019, 10, 1114.	1.1	39
18	CCM1 and CCM2 variants in patients with cerebral cavernous malformation in an ethnically Chinese population in Taiwan. Scientific Reports, 2019, 9, 12387.	1.6	5

#	Article	IF	CITATIONS
19	A longitudinal fixel-based analysis of white matter alterations in patients with Parkinson's disease. Neurolmage: Clinical, 2019, 24, 102098.	1.4	35
20	Exploring the Spectrum of Subcortical Hyperintensities and Cognitive Decline. Journal of Neuropsychiatry and Clinical Neurosciences, 2018, 30, 130-138.	0.9	8
21	Cortical damage in the posterior visual pathway in patients with sialidosis type 1. Brain Imaging and Behavior, 2017, 11, 214-223.	1.1	7
22	Apolipoprotein E Genotype and Sex Risk Factors for Alzheimer Disease. JAMA Neurology, 2017, 74, 1178.	4.5	454
23	Multiparametric imaging using 18F-FDG PET/CT heterogeneity parameters and functional MRI techniques: prognostic significance in patients with primary advanced oropharyngeal or hypopharyngeal squamous cell carcinoma treated with chemoradiotherapy. Oncotarget, 2017, 8, 62606-62621.	0.8	30
24	Predictive value of 1H MR spectroscopy and 18F-FDG PET/CT for local control of advanced oropharyngeal and hypopharyngeal squamous cell carcinoma receiving chemoradiotherapy: a prospective study. Oncotarget, 2017, 8, 115513-115525.	0.8	2
25	Myocardial triglyceride content at 3ÂT cardiovascular magnetic resonance and left ventricular systolic function: a cross-sectional study in patients hospitalized with acute heart failure. Journal of Cardiovascular Magnetic Resonance, 2016, 18, 9.	1.6	14
26	Dynamic contrast-enhanced MRI, diffusion-weighted MRI and 18F-FDG PET/CT for the prediction of survival in oropharyngeal or hypopharyngeal squamous cell carcinoma treated with chemoradiation. European Radiology, 2016, 26, 4162-4172.	2.3	55
27	Alterations of diffusion tensor MRI parameters in the brains of patients with Parkinson's disease compared with normal brains: possible diagnostic use. European Radiology, 2016, 26, 3978-3988.	2.3	10
28	Increased Water Diffusion in the Parcellated Cortical Regions from the Patients with Amnestic Mild Cognitive Impairment and Alzheimer's Disease. Frontiers in Aging Neuroscience, 2016, 8, 325.	1.7	9
29	Probability-based prediction model using multivariate and LVQ-PNN for diagnosing dementia. Neuropsychiatry, 2016, 06, .	0.4	1
30	Clinical Utility of Multimodality Imaging with Dynamic Contrast-Enhanced MRI, Diffusion-Weighted MRI, and 18F-FDG PET/CT for the Prediction of Neck Control in Oropharyngeal or Hypopharyngeal Squamous Cell Carcinoma Treated with Chemoradiation. PLoS ONE, 2014, 9, e115933.	1.1	53
31	Tract-Based Spatial Statistics: Application to Mild Cognitive Impairment. BioMed Research International, 2014, 2014, 1-8.	0.9	9
32	Magnetic-resonance imaging for kinetic analysis of permeability changes during focused ultrasound-induced blood–brain barrier opening and brain drug delivery. Journal of Controlled Release, 2014, 192, 1-9.	4.8	54
33	Brain connectivity of patients with Alzheimer's disease by coherence and cross mutual information of electroencephalograms during photic stimulation. Medical Engineering and Physics, 2013, 35, 241-252.	0.8	10
34	Noninvasive Monitoring of Microvascular Changes With Partial Irradiation Using Dynamic Contrast-Enhanced and Blood Oxygen Level-Dependent Magnetic Resonance Imaging. International Journal of Radiation Oncology Biology Physics, 2013, 85, 1367-1374.	0.4	17
35	Pharmacodynamic Analysis of Magnetic Resonance Imaging-Monitored Focused Ultrasound-Induced Blood-Brain Barrier Opening for Drug Delivery to Brain Tumors. BioMed Research International, 2013, 2013, 1-13.	0.9	31
36	Magnetic Resonance Imaging of Mouse Islet Grafts Labeled with Novel Chitosan-Coated Superparamagnetic Iron Oxide Nanoparticles. PLoS ONE, 2013, 8, e62626.	1.1	14

#	Article	IF	CITATIONS
37	Dynamic Contrast-Enhanced MR Imaging Predicts Local Control in Oropharyngeal or Hypopharyngeal Squamous Cell Carcinoma Treated with Chemoradiotherapy. PLoS ONE, 2013, 8, e72230.	1.1	49
38	Sex dimorphism of cortical water diffusion in normal aging measured by magnetic resonance imaging. Frontiers in Aging Neuroscience, 2013, 5, 71.	1.7	7
39	Discrimination between Alzheimer's Disease and Mild Cognitive Impairment Using SOM and PSO-SVM. Computational and Mathematical Methods in Medicine, 2013, 2013, 1-10.	0.7	31
40	Diffusion Magnetic Resonance Imaging and Its Applications in Movement Disorders. , 2013, , 49-58.		0
41	Cortical involvement in a gait-related imagery task: Comparison between Parkinson's disease and normal aging. Parkinsonism and Related Disorders, 2012, 18, 537-542.	1.1	51
42	Blind estimation of the arterial input function in dynamic contrastâ€enhanced MRI using purity maximization. Magnetic Resonance in Medicine, 2012, 68, 1439-1449.	1.9	16
43	Vascularization and restoration of heart function in rat myocardial infarction using transplantation of human cbMSC/HUVEC core-shell bodies. Biomaterials, 2012, 33, 2127-2136.	5.7	30
44	Injectable PLGA porous beads cellularized by hAFSCs for cellular cardiomyoplasty. Biomaterials, 2012, 33, 4069-4077.	5.7	60
45	Parkinson Disease: Diagnostic Utility of Diffusion Kurtosis Imaging. Radiology, 2011, 261, 210-217.	3.6	213
46	18F-FDG PET/CT and 3.0-T whole-body MRI for the detection of distant metastases and second primary tumours in patients with untreated oropharyngeal/hypopharyngeal carcinoma: a comparative study. European Journal of Nuclear Medicine and Molecular Imaging, 2011, 38, 1607-1619.	3.3	51
47	Characterization of quaternized chitosanâ€stabilized iron oxide nanoparticles as a novel potential magnetic resonance imaging contrast agent for cell tracking. Polymer International, 2011, 60, 945-950.	1.6	25
48	Preparation, characterization and application of superparamagnetic iron oxide encapsulated with N-[(2-hydroxy-3-trimethylammonium) propyl] chitosan chloride. Carbohydrate Polymers, 2011, 84, 781-787.	5.1	19
49	Enhancement of cell retention and functional benefits in myocardial infarction using human amniotic-fluid stem-cell bodies enriched with endogenous ECM. Biomaterials, 2011, 32, 5558-5567.	5.7	81
50	Clinical significance of the pallidoreticular pathway in patients with carbon monoxide intoxication. Brain, 2011, 134, 3632-3646.	3.7	40
51	Multi-parametric neuroimaging evaluation of cerebrotendinous xanthomatosis and its correlation with neuropsychological presentations. BMC Neurology, 2010, 10, 59.	0.8	27
52	Selfâ€Assembled pH‧ensitive Nanoparticles: A Platform for Oral Delivery of Protein Drugs. Advanced Functional Materials, 2010, 20, 3695-3700.	7.8	104
53	Microstructural changes in patients with progressive supranuclear palsy: A diffusion tensor imaging study. Journal of Magnetic Resonance Imaging, 2010, 32, 69-75.	1.9	55
54	In situ preparation of high relaxivity iron oxide nanoparticles by coating with chitosan: A potential MRI contrast agent useful for cell tracking. Journal of Magnetism and Magnetic Materials, 2010, 322, 208-213.	1.0	88

#	Article	IF	CITATIONS
55	The characteristics, biodistribution, magnetic resonance imaging and biodegradability of superparamagnetic core–shell nanoparticles. Biomaterials, 2010, 31, 1316-1324.	5.7	87
56	<i>In vivo</i> Assessment of Macrophage CNS Infiltration during Disruption of the Blood–Brain Barrier with Focused Ultrasound: A Magnetic Resonance Imaging Study. Journal of Cerebral Blood Flow and Metabolism, 2010, 30, 177-186.	2.4	28
57	Blood-Brain Barrier Disruption with Focused Ultrasound Enhances Delivery of Chemotherapeutic Drugs for Glioblastoma Treatment. Radiology, 2010, 255, 415-425.	3.6	337
58	Novel magnetic/ultrasound focusing system enhances nanoparticle drug delivery for glioma treatment. Neuro-Oncology, 2010, 12, 1050-1060.	0.6	115
59	Magnetic resonance monitoring of focused ultrasound/magnetic nanoparticle targeting delivery of therapeutic agents to the brain. Proceedings of the National Academy of Sciences of the United States of America, 2010, 107, 15205-15210.	3.3	351
60	Longitudinal study of carbon monoxide intoxication by diffusion tensor imaging with neuropsychiatric correlation. Journal of Psychiatry and Neuroscience, 2010, 35, 115-125.	1.4	40
61	Focused ultrasound induced blood-brain barrier disruption to enhance chemotherapeutic drugs (BCNU) delivery for glioblastoma treatment. , 2010, , .		6
62	Computer-Aided Diagnosis of Alzheimer's Disease Using Multiple Features with Artificial Neural Network. Lecture Notes in Computer Science, 2010, , 699-705.	1.0	9
63	An Image-Aided Diagnosis System for Dementia Classification Based on Multiple Features and Self-Organizing Map. Lecture Notes in Computer Science, 2010, , 462-469.	1.0	2
64	Myometrial Invasion in Endometrial Cancer: Diagnostic Accuracy of Diffusion-weighted 3.0-T MR Imaging—Initial Experience. Radiology, 2009, 250, 784-792.	3.6	164
65	Magnetic resonance imaging enhanced by superparamagnetic iron oxide particles: Usefulness for distinguishing between focused ultrasoundâ€induced blood–brain barrier disruption and brain hemorrhage. Journal of Magnetic Resonance Imaging, 2009, 29, 31-38.	1.9	45
66	Potential in reducing scan times of HARDI by accurate correction of the crossâ€ŧerm in a hemispherical encoding scheme. Journal of Magnetic Resonance Imaging, 2009, 29, 1386-1394.	1.9	8
67	Correlation of apparent diffusion coefficients measured by 3T diffusion-weighted MRI and SUV from FDG PET/CT in primary cervical cancer. European Journal of Nuclear Medicine and Molecular Imaging, 2009, 36, 200-208.	3.3	109
68	Pretreatment evaluation of distant-site status in patients with nasopharyngeal carcinoma: accuracy of whole-body MRI at 3-Tesla and FDG-PET-CT. European Radiology, 2009, 19, 2965-2976.	2.3	38
69	Cortical control of gait in healthy humans: an fMRI study. Journal of Neural Transmission, 2008, 115, 1149-1158.	1.4	73
70	Detection of lymph node metastasis in cervical and uterine cancers by diffusionâ€weighted magnetic resonance imaging at 3T. Journal of Magnetic Resonance Imaging, 2008, 28, 128-135.	1.9	213
71	Visualization of the coherence of the principal diffusion orientation: An eigenvectorâ€based approach. Magnetic Resonance in Medicine, 2008, 59, 764-770.	1.9	13
72	Hemorrhage Detection During Focused-Ultrasound Induced Blood-Brain-Barrier Opening by Using Susceptibility-Weighted Magnetic Resonance Imaging. Ultrasound in Medicine and Biology, 2008, 34, 598-606.	0.7	124

#	Article	IF	CITATIONS
73	The cortical modulation from the external cues during gait observation and imagination. Neuroscience Letters, 2008, 443, 232-235.	1.0	20
74	Reduced Encoding Diffusion Spectrum Imaging Implemented With a Bi-Gaussian Model. IEEE Transactions on Medical Imaging, 2008, 27, 1415-1424.	5.4	16
75	Determination of Fiber Orientation in MRI Diffusion Tensor Imaging Based on Higher-Order Tensor Decomposition. Annual International Conference of the IEEE Engineering in Medicine and Biology Society, 2007, 2007, 2065-8.	0.5	5
76	The effects of single-trial averaging on the temporal resolution of functional MRI. Magnetic Resonance Imaging, 2006, 24, 597-602.	1.0	4
77	Novel diffusion anisotropy indices: An evaluation. Journal of Magnetic Resonance Imaging, 2006, 24, 211-217.	1.9	16
78	Selective averaging for the diffusion tensor measurement. Magnetic Resonance Imaging, 2005, 23, 585-590.	1.0	6
79	3D DT-MRI using a reduced-FOV approach and saturation pulses. Magnetic Resonance in Medicine, 2004,	1.9	10